High power neon seeded JET discharges: Experiments and simulations

High power neon seeded JET discharges: experiments and simulations

G. Telesca [1], I. Ivanova-Stanik[2], R. Zagórski [2], S. Brezinsek [3], P. Drewelow [4], C. Giroud [5], A. Huber [3], S. Wiesen [3], M .Wischmeier [6] and JET contributors[*]
EUROfusion Consortium, JET, Culham Science Centre, Abingdon, OX14 3DB, UK

[1]*Department of Applied Physics, Ghent University, B-9000 Gent, Belgium*
[2] *Institute of Plasma Physics and Laser Microfusion, Warsaw, Poland*
[3] *Institut fuer Energie-und Klimaforschung-Plasmaphysik Foschungszentrum Juelich GmbH, Juelich, Germany.*
[4]*Max-Planck Institut fuer Plasmaphysik D-17491 Greifswald, Germany.*
[5]*CCFE Culham, Abingdon, Oxon. OX14 3DB, UK*
[6]*Max-Planck Institut fuer Plasmaphysik D-85748, Garching bei Muenchen, Germany.*

Abstract

A series of neon seeded JET ELMy H-mode pulses is considered from the modeling as well as from the experimental point of view. For two different Ne seeding rates and two different D puffing gas levels the heating power, P_{heat}, is in the range 22-29.5 MW. The main focus is on the numerical reconstruction of the total radiated power (which mostly depends on the W concentration) and its distribution between core and divertor and of *Zeff* (which mostly depends on the Ne concentration). To model self-consistently the core and the SOL two input parameters had to be adjusted case by case: the SOL diffusivity, D_{SOL}, and the core impurity inward pinch, v_{pinch}. D_{SOL} had to be increased with increasing Γ_{Ne} and the level of v_{pinch} had to be changed, for any given Γ_{Ne}, according to the level of P_{heat}: it decreases with increasing P_{heat}. Since the ELM frequency, f_{ELM}, is experimentally correlated with P_{heat}, (it increases with P_{heat}) the impurity inward pinch can be seen as to depend on f_{ELM}. Therefore, to maintain a low v_{pinch} level (i.e. high f_{ELM}) Γ_{Ne}/P_{heat} should not exceed a certain threshold, which slightly increases with the Γ_D rate. This might lead to a limitation in the viability of reducing the target heat load by Ne seeding at moderate Γ_D, while keeping *Zeff* at acceptably low level.

[*] *see the Appendix of F. Romanelli et al., Proceedings of the 25th IAEA Fusion Energy Conference 2014, Saint Petersburg, Russia.*

1.Introduction

For a fully metallic device like JET with the ITER-Like-Wall (W divertor, Be wall) impurity seeding is an essential technique to reduce the power load to the targets, via enhanced edge radiation. Indeed, the naturally occurring radiation losses are low (~ 25-30 % of the heating power), as compared to those with carbon target (~ 50 %). Significant progress has been made at JET in reducing the heat and particle load to the divertor plates by injecting light impurities as N, Ne and Ar, expecially in the ITER-relevant vertical-target configuration (low and high delta), at I_p= 2.5 MA and B_t = 2.7 T [1,2].

In contrast to Ne injection with carbon PFC, Ne seeding in ILW causes significant changes in the radiation pattern also in the core plasma. Generally, Ne injection not only leads to enahanced radiation in the SOL and around the X-point, as for carbon sorroundings, but also to increased tungsten release, with related enhanced core radiation and possible reduced ELM frequency. This can cause excessive impurity resilience time and may lead to impurity accumulation [3]. This paper, based on experimental JET data as well as on core-SOL self-consistent modelling, is focusing on the relation between the level of Ne seeding rate and the change in the impurity transport.

Among a number of experiments carried out recently, a series of Ne seeded low-delta ELMy H-mode pulses with heating power, P_{heat}, up to 29.5 MW and with two different levels of seeding rate as well of gas fueling is considered in the present study.

We have focused our interest on the global radiation properties of these pulses as well as on impurity transport and on *Zeff*, neglecting other aspects of these discharges, as, for example, the confinement properties (see ref.[1,2,4]). In particular, an anomalously high *Zeff* is observed to occour when, for a given level of P_{heat}, Ne seeding exceeds a certain threshold. In this case, indeed, the incremental *Zeff* caused by Ne seeding is higher than that expected from the related incremental radiated power. It is also observed that the ELM activity decreases significantly, while the plasma enegy remains unchanged.

In these pulses the volume average density, $\langle n_e \rangle$, is in the range 6-7 x $10^{19}/m^3$, P_{heat} from 22 to 29.5 MW (NBI+ICRH), the two steps in Ne seeding rate are 5 and 12 x 10^{21} e/s and the two steps in D_2 gas fuelling rate are 1.9 and 3.7 x 10^{22}/s. The radiated power fraction ($frad = P_{rad}^{TOT} / P_{heat}$) changes from 0.47 to 0.61 and the ratio of radiated power in the SOL to the

total one (P_{rad}^{SOL} / P_{rad}^{TOT}) is between 0.35 and 0.43. The main aim of this work consists in reproducing numerically, for each pulse, the electron temperature, $T_e(r)$, and density $n_e(r)$ profiles, in the core plasma, P_{rad}^{TOT} , $P_{rad}^{SOL}/P_{rad}^{TOT}$ and *Zeff* by changing a limited number of inputs : $<n_e>$, P_{heat} and Γ_{Ne} (see next section). It is worth mentioning that for each ¨shot-point¨ the simulation outputs shown in Sect. 3 are obtained from a single run, i.e. all the quantities are calculated simultaneously. Indeed, numerical simulation of these discharges is being made in view of finding the best conditions leading to high f_{rad} together with acceptable *Zeff* for a situation as close as possible to a real experimental pulse,

For the simulations we have used COREDIV code [5], which self-consistently couples the plasma core (1-D) with the plasma edge (2-D) and the main plasma with impurities. Although the simulations refer to the inter-ELM phase of the discharges, since production as well as flushing out of W due to ELMs is not accounted for in the present model, the numerical results might be compared with experimental data averaged over several ELM periods [6,7].

Section 2 deals with the description of the numerical model COREDIV. In Sect. 3 the numerical results are compared with experimental data. Discussion and summary are made in Sect.4.

2 The COREDIV code

Since the energy balance depends strongly on the coupling between the bulk and the scrape-off layer (SOL) plasma, modeling requires the transport problem to be addressed in both regions simultaneously. The physics model used in the COREDIV code is based on a self-consistent coupling of the radial transport in the core to the 2D multifluid description of the SOL.

In the core, given as code input the volume average electron density $<n_e>$, the 1D radial transport equations for bulk ions, for each ionization state of impurity ions and for the electron and ion temperature are solved. The electron and ion energy fluxes are defined by the local transport model proposed in ref. [8] which reproduces a prescribed energy confinement law. In particular, the anomalous heat conductivity is given by the expression $\chi_{e,i} = C_{e,i} * a^2/\tau_E * F(r)$ where r is the radial coordinate, a is the plasma radius, τ_E is the energy confinement time defined by the ELMy H-mode scaling law and the coefficient ($C_e = C_i$) is adjusted to have agreement between calculated and experimental confinement times.

The parabolic-like profile function $F(r)$, which may slightly change from run to run in order to match with the actual profiles of the experimental pulse to be modelled, can be modified at the plasma edge to provide for a transport barrier of chosen level. The main plasma ion density is given by the solution of the radial diffusion equation with diffusion coefficients $D_i = D_e = 0.2\chi_e$, as in ref.[8]. Note, however, that the solution of the diffusion equation is largely independent of the exact value of D_e/χ_e. Indeed, a change in D_e/χ_e causes a consistent change in the source term, since the average electron density is a COREDIV input. For the auxiliary heating, parabolic-like deposition profile is assumed $P_{aux}(r) = P_0 (1-r^2/a^2)^y$ where y is in the range 1.5-3, depending on the quality of the auxiliary heating, NBI or/and ICRF. For all the pulses considered in this study y=2, since the fraction of ICRH power level to the total power is nearly constant, P_{ICRH}/P_{NBI} = 0.2. The impurity diffusion coefficient is set to be equal to that of the main ions and an anomalous impurity pinch is given as input, in the range 0 to -1 m/s for the pulses here considered (see Sect.3).

In the SOL the 2D boundary layer code EPIT is used, which is primarily based on Braginskii-like equations for the background plasma and on rate equations for each ionization state of each impurity species. An analytical description of the neutrals is used, based on a simple diffusive model. COREDIV takes into account the plasma (D, Be and seeded impurities) recycling in the divertor as well as the sputtering processes at the target plates including W sputtering by deuterons, self-sputtering and sputtering due to seeded impurities. (For deuterium and neon sputtering and tungsten self-sputtering the yields given in refs. [9,10] are used). The recycling coefficient is an external parameter which in COREDIV depends on the level of the electron density at the separatrix, n_{e_sep}, given as an input, and increases with increasing n_{e_sep}.

A simple slab geometry (poloidal and radial directions) with classical parallel transport and anomalous radial transport ($D_{SOL} = \chi_i = 0.5\ \chi_e$, where χ_e ranges typically 0.5-1.5 m^2/s), is used and the impurity fluxes and radiation losses by impurity ions are calculated fully self-consistently. Although the values of the transport coefficients in the SOL are generally quite comparable to those at the separatrix, in the present simulations the value of D_{SOL} is set arbitrarily (in the range 0.4-0.7 m^2/s) in order to match with the core-SOL distribution of the radiated power, depending on the different levels of Ne seeding rate (see next section). All the equations are solved only from the midplane to the divertor plate, assuming inner-outer

symmetry of the problem. This implies that the experimental in–out asymmetries, observed especially at high density-high radiation level, are not reproduced in COREDIV results. However, for all the different situations examined so far (with carbon plates and with the ILW, and with different seeding levels [6,11]) the COREDIV numerical reconstructed total radiation in the SOL matches well with the total experimentally measured SOL radiation, indicating that for JET conditions the edge-core COREDIV model can describe the global trend of this important quantity.

The coupling between the core and the SOL is made by imposing continuity of energy and particle fluxes as well as of particle densities and temperatures at the separatrix. The computed fluxes from the core are used as boundary condition for the SOL plasma. In turn, the values of temperatures and of densities calculated in the SOL are used as boundary conditions for the core module

3. Experiments and simulations

Fig.1 shows some time-dependent traces of the four pulses under exam. In JPN 87190 (top left) P_{heat} (NBI +RF) is 22MW, Γ_{Ne} = 0.5 10^{22}e/s and for t < 14.5 s with Γ_D =4.0 x 10^{22} e/s ELM activity is stationary with f_{ELM}=40 Hz, *Zeff*=1.9 and f_{RAD} =0.47. Starting from t=14.5s the gas fueling decreses to Γ_D =1.9x 10^{22} e/s and the ELM behavior is non-stable, alternating periods of ELM activity with f_{ELM}= 40 Hz with ELMy-free periods. Correlated also with a slight decrease in $\langle n_e \rangle$, *Zeff* goes up to 2.4 and f_{RAD}=0.52. In JPN 87191 (top right) the two gas fuelling steps are interchanged in time, but their values are quite similar to those in the previous pulse, while remains Γ_{Ne} = 0.5 10^{22}e/s. With P_{heat} = 26 MW, ELM activity is stable at both Γ_D, f_{ELM} = 60-70 Hz, with *Zeff* around 2 and f_{RAD} =0.54 and 0.47 respectively. In JPN 87192 (bottom left), Γ_{Ne}=1.2 10^{22}e/s while all the other inputs are keept as in the previous pulse. ELM activity is non-stable with f_{ELM}= 5-9 Hz, *Zeff* in the range 3.4-3.0 and f_{RAD} around 0.55. Adding 1 MW of ICRH, as in JPN 87194 (bottom right) up to t=14.5s, does not improve the situation with respect to *Zeff* and f_{ELM}. At t=14.5s, 2 more megawatts NBI are added resulting in P_{heat} = 29.5 MW. Even though no significant improvement is observed with respect to *Zeff*, a tendency towards a more regular ELM behavior might be seen, with f_{ELM} which becomes 15Hz. A summary of the experimental data for the 7 time slices (“shot-

points") belonging to the 4 pulses examined is given in table I. In the following, comparison is made between the experimental data of table I and COREDIV numerical results.

Before comparing and discussing the global quantilties of the core and the SOL, the experimental (from High Resolution Thomson Scattering diagnostic) and simulated T_e and n_e profiles in the core plasma of one of the four pulses here considered (JPN 87194 t= 14.9 s) are shown in Fig. 2, as an example. Although some discrepancies experiment-simulation can be seen, these discrepancies are marginally influent for the numerical reconstruction of the global quantities of the core plasma, due to the flatness of the n_e profile.

Fig.3a shows the tomographic reconstruction from bolometric data for one typical Ne seeded JET pulse. It is apparent that a clear limit between the radiation emitted in the core and that in the SOL is difficult to define within the uncertainties in space and absolute numbers of the measurement (order of 20%), especially in the vicinity of the x-point. Therefore, we have followed a procedure, used at JET [12], by which all the power radiated below Z= -1 m is considered as divertor radiation. Since neon radiates partly in the SOL and partly at the very edge of the plasma core around the X-point, this assumption turns out to include the total radiation emitted by Ne in what we call "experimental divertor radiation". Being the core module of COREDIV one-dimensional (see above), the simulated Ne radiation inside the separatrix is poloidally uniformly distributed and it is located, as in the experiment, at the very edge of the core (see Fig. 3b). To compare consistently simulations with measurements we have therefore added the COREDIV neon radiation emitted at the very edge of the core to the COREDIV SOL radiation, resulting in the "simulated divertor radiation". In Fig. 4 the seven "shot-points" have been ordered according to P_{heat} and the four points referring to *Pheat*=26 MW have been slithly displaced in P_{heat} to avoid superposition. The points referring to Γ_{Ne}=1.2 10^{22}e/s have been drawn with larger symbols. Fig.4a,b show that both P_{rad}^{TOT} and P_{rad}^{SOL} / P_{rad}^{TOT} have been numerically reconstructed with sufficient accuracy while the reconstructed *Zeff* (Fig.4c) is systematically a little under-estimated in the simulations. This is possibly due to the absence of impurities like C, O and Ni in the presently performed COREDIV runs. Fig.4d shows that the experimental f_{RAD} (as well as the simulated one) does not increase significantly by increasing Γ_{Ne} , which, however, leads to a clear increase in *Zeff*. This point is made more clear by noting that the quantity P_{rad}^{TOT} / (*Zeff*-1) x n_e^2 [13] drops nearly by a factor of 2 at high Γ_{Ne} (Fig.4e). Figs. 4f and 4g show that

the reconstructed average W and Ne concentration match well with the experimental ones, considering the error bar (order 20%) of the measurements. The electron temperature at the outer stike point, measured by LP (with significant error bar), is in the range 6-9 eV (9 eV for the pulse at 26 MW with Γ_{Ne} = 0.5x10^{22} e/s), while the simulated one is in the range 4-6.5 eV. Considering that the experimental T_e at the inner strike point is about 2-3 eV lower than at outer one, the discrepancy experiment-simulation is consistent with the COREDIV SOL model, in which in-out symmetry is assumed (only one target plate, see Sect. 2). Fig.4h shows that high Γ_{Ne} level is an effective tool to reduce the power to the plate also at high P_{heat}. The simulated recycling D fluxes, Γ_D, are about a factor of 2 higher than the LP experimental ones. This depends on the value of the COREDIV input electron density at the separatrix, n_{e_sep}. Indeed, the recycling deuterium flux is not a free parameter in the model (see Sect.2), but it is linked to the input value of n_{e_sep}, which, in all these simulations has been set as n_{e_sep}=0.45 <n_e>. [6]

Together with P_{heat} , <n_e> and Γ_{Ne} two other input parameters have been changed "shot-point" to "shot-point" in order to match simulations with experiments: D_{SOL} and the anomalous impurity pinch, v_{pinch}. Differently from modelling of unseeded pulses with D_{SOL} =0.25 m^2/s, it has been set D_{SOL} =0.45 m^2/s for the points at Γ_{Ne}=0.5x10^{22}e/s and D_{SOL} up to 0.70 m^2/s for the points at Γ_{Ne}=1.2x 10^{22}e/s. This dependence of D_{SOL} on the level of Γ_{Ne} is made to match the simulated with the experimental P_{rad}^{SOL}. To match both the simulated P_{rad}^{core} (i.e. P_{rad}^{TOT} - P_{rad}^{SOL}) and *Zeff* with the experimental data, v_{pinch} had to be changed in the range ~ - 0.3 - 0.8 m/s. It turns out that v_{pinch} is correlated with f_{ELM}, as seen in Fig. 5a. It has to be pointed out, however, that there is no experimental evidence of change in impurity density peaking with decreasing f_{ELM} and that the T_e profile is centrally peaked for all these (partly) RF centrally heated plasmas, while the n_e profile is flat. Considering, moreover, that v_{pinch} is a numerical tool introduced to change the impurity dwell time, a different approach has been sought to account for the increased *Zeff* at low f_{ELM}. In fact, a new set of simulations has been performed in which the impurity inward pinch is keept constant (v_{pinch} = - 0.3 m/s) for all the seven shot points and machting between experiments and simulations is searched by adjusting the impurity diffusion coefficient in the core plasma, $D_{imp\text{-}core}$. In all the simulations previously reported the impurity diffusivity in the core plasma is set to be equal to that of the main ions, $D_{imp\text{-}core}$ = $D_{main\ ions}$, while in the new set of simulations $D_{imp\text{-}}$

$_{core}$/$D_{main\text{-}ions}$ has been scanned to find the best match experiments-simulations. The numerical results previously reported, as in Fig. 4, have been fairly well reproduced applying values of $D_{imp\text{-}core}/D_{main\ ions}$, which decrase with decreasing f_{ELM}, Fig, 5b. Recalling that in the COREDIV model $D_{main\ ions} = D_e = 0.2\chi_e$ the decrease in $D_{imp\text{-}core}/D_{main\ ions}$ implies an increase in τ_{imp}/τ_E, where τ_{imp} is the impurity dwell time.

Since the key parameters of this study are Γ_{Ne}, P_{heat} and Γ_D, the seven data points above considered plus two from JPN 87194 at t< 14 s and three points belonging to a quite similar series with P_{heat}= 24 MW and Γ_D = 4.1 x 10^{22} el/s (JPN 87090-92 [7]) have been labelled according to their value of Γ_{Ne}/P_{heat} and plotted as function of Γ_D, Fig 6. Although it is not possible to draw any quantitative dependence from these data, the plot shows the positive effect of the gas puffing rate on enhancing the level of Γ_{Ne}/P_{heat} for which f_{ELM} remains in excess of 40 Hz.

4. Discussion and summary.

Using the actual steady-state version of COREDIV it is not possible to simulate the effect on W release caused by single ELMs. However, for T_{e_pl} above 3-4 eV the W sputtering yield by Ne together with that by Be and by W self-sputtering provide a simulated W flux, which is comparable to that experimentally observed for the most common JET ELMy H-mode situations, once the data are averaged over times $\tau_A >> 1/f_{ELM}$ [6]. Indeed, in JET ELMy-H mode the experimental Γ_W is found to be in the range 3-9x10^{19}/s [14,15], as in COREDIV simulations. In particular, for this series of pulses the intensity of the WI emission line at 401 nm, measured at the outer divertor, shows a slight increase (up to about 30 %) with increasing Γ_{Ne}, in line with the calculated COREDIV total W fluxes, which increase from about 7 to 9.5 x 10^{19}/s.

The necessity of introducing in the simulations an anomalous inward pinch (or an "*ad hoc*" decrease in the impurity diffusion coefficient) to match experiment-simulation for the pulses at low f_{ELM} is correlated with the impurity flushing out mechanisms by ELMs [16], and, specifically, with the experimentally observed decrease in W density in the core plasma for f_{ELM} above 40 Hz [15]. In fact, ELMs are simultaneously the main cause of W release and of impuritiy outflow [17].

Taking 40 Hz as the minimal f_{ELM} for impurity (Ne and W) accumulation avoidance and considering that for these JET pulses τ_E is 0.15-0.2 s , the resulting τ_E x f_{ELM} is 6-8, which is not far from the value of 10, found in previous studies as the minimal τ_E x f_{ELM} to avoid W accumulation [17,18].

In spite of the inner-outer symmetry assumption and of the analytical description of the neutrals which both might hamper the validity of the SOL model especially for situations close to detachment, the global properties of the SOL, as the radiated power and by consequence the average electron temperature at the plate, are sufficiently well numerically reproduced, due also to the adjustement of the particle diffusion coefficient in the SOL, D_{SOL}. The change in D_{SOL} is a technical tool to fitting the numerical P_{rad}^{SOL} with the experimental one and although it reflects the increase in collisionality with decreasing the divertor temperature it includes also the action of other mechanisms as change in frictional forces and in flux expansion [1].

Experiments and COREDIV modelling indicate that Ne seeding is an efficient method to maintain the power load to the target plates at acceptable level also at high P_{heat} (order 30 MW) in JET-ILW pulses. However, the level of Γ_{Ne} should be modulated according to the level of Γ_D and of P_{heat} to maintain *Zeff* at acceptable values. Indeed, when for given Γ_D and P_{heat} the neon seeding rate exceeds a certain treshold, COREDIV simulations indicate that an inward impurity pinch (order -1 m/s) is triggered (or, alternatively, a decrease in the core impurity diffusivity), esperimentally related to the reduction of ELM activity and to a significant *Zeff* increase. There is no clear reason for this change in impurity transport since also for the pulses at the highest Γ_{Ne} (P_{heat} =26 and 29.5 MW) the power crossing the separatrix (P_{SOL} in Fig. 4h) is well above the H-L back transition, about 8 MW. (Note that in Fig. 4h P_{SOL} is calculated summing up all the losses inside the separatrix, including Ne radiation in the confined plasma). To this point it is worth recalling that the “shot points” at lowest f_{ELM} are experimentally correlated to the highest Γ_{Ne} / P_{aux} as well as to the highest confinement enhancement factor, H_{98}.

In conclusion, even though the simplifying assumptions made in COREDIV in order to model self-consistently the complex interaction core-edge plasma certainly attenuate the validity of some quantitative numerical results, the simulation of the pulses here considered indicates a clear trend and suggests a possible limit in the level of Γ_{Ne} / P_{aux} (hence in f_{RAD}) at

moderate gas puffing rate, if the decrease in ELM activity and the related increase in impurity dwell time is to be avoided. This, of course, refers only to the case of uncontrolled (natural) ELM frequency.

Acknowledgements

This work has been carried out within the framework of the EUROfusion Consortium and has received funding from the Euratom research and training programme 2014-2018 under grant agreement No 633053. The views and opinions expressed herein do not necessarily reflect those of the European Commission.

This scientific work was financed within the Polish framework of the scientific financial resources allocated for realization of the international co-financed project.

References

[1] M. Wischmeier, J. Nucl. Mater. **463** (2015) 22 *and* 25th IAEA Conference 2014, P. EX/7-2, St. Petersburg, Russia.

[2] C. Giroud et al., Nucl. Fusion **53** (2013) 113025 *and* 25th IAEA Conference 2014. EX/P5-25, St. Petersburg, Russia.

[3] T. Puetterich et al., Plasma Phys. Control. Fusion **55** (2013)124036]

[4] A. Huber et al., J. Nucl. Mater. **463** (2015) 445

[5] R. Zagorski, et al., Nucl. Fusion **53** (2013) 073030

[6] G.Telesca et al., Contrib. Plasma Phys. **54,** issue 4–6 (2014) 347-352/DOI 10.1002/ctpp.201410052

[7] G. Telesca *et al.* J. Nucl. Mater. **463** (2015) 577-581 doi:10.1016/j.jnucmat.2014.11.024

[8] J. Mandrekas and W.M. Stacey, Nucl. Fusion **35** (1995) 843

[9] Y.Yamamura et al., Report of the IPP Nagoya, IPPJ-AM-26 (1083)

[10] C. Garcia-Rosales et al., J. Nucl. Mater. **218** (1994) 8-17

[11] G. Telesca et al., Plasma Phys. Control. Fusion **53** (2011) 115002

[12] A. Huber et al., 41st EPS Conference on Plasma Physics (2014), P1.031

[13] G. Telesca et al., Nucl. Fusion **40** (2000) 1845

[14] S. Brezinsek et al., 57th APS Plasma Physics, Savannah (2015), Vol.60, N. 19, T06.0007

[15] N. den Harder et al., Nucl. Fusion **56** (2016) 026014

[16] R. Dux et al., J. Nucl. Mater. **390-391**(2009) 85

[17] A. Loarte et al., Nucl. Fusion **54** (2014) 033007

[18] R. Dux et al., Nucl. Fusion **51** (2011) 053002

.

Figure captions

Fig.1. Experimental time traces of the four pulses examined. The seven time slices of the simulated "shot points" are shown.

Fig.2. Experimental (HRTS) and reconstructed T_e and n_e profiles for JPN 87194 t=14.9 s.

Fig.3. a)Tomographic reconstruction of the radiated power density for a typical neon seeded JET pulse at high P_{heat}, JPN 87194 t= 15s. b) COREDIV simulated radiated power density profile by neon inside the separatrix.

Fig. 4. Comparison experiment-simulation for the seven "shot points" here considered.

Fig.5. a) Numerical pinch velocity vs. experimental ELM frequency. b) Numerical D_{imp}/D_{main} in the core plasma vs. experimental ELM frequency

Fig.6. Experimental Γ_{Ne}/P_{heat} vs Γ_D with different symbols for f_{ELM} > 40 Hz and f_{ELM} <20Hz.

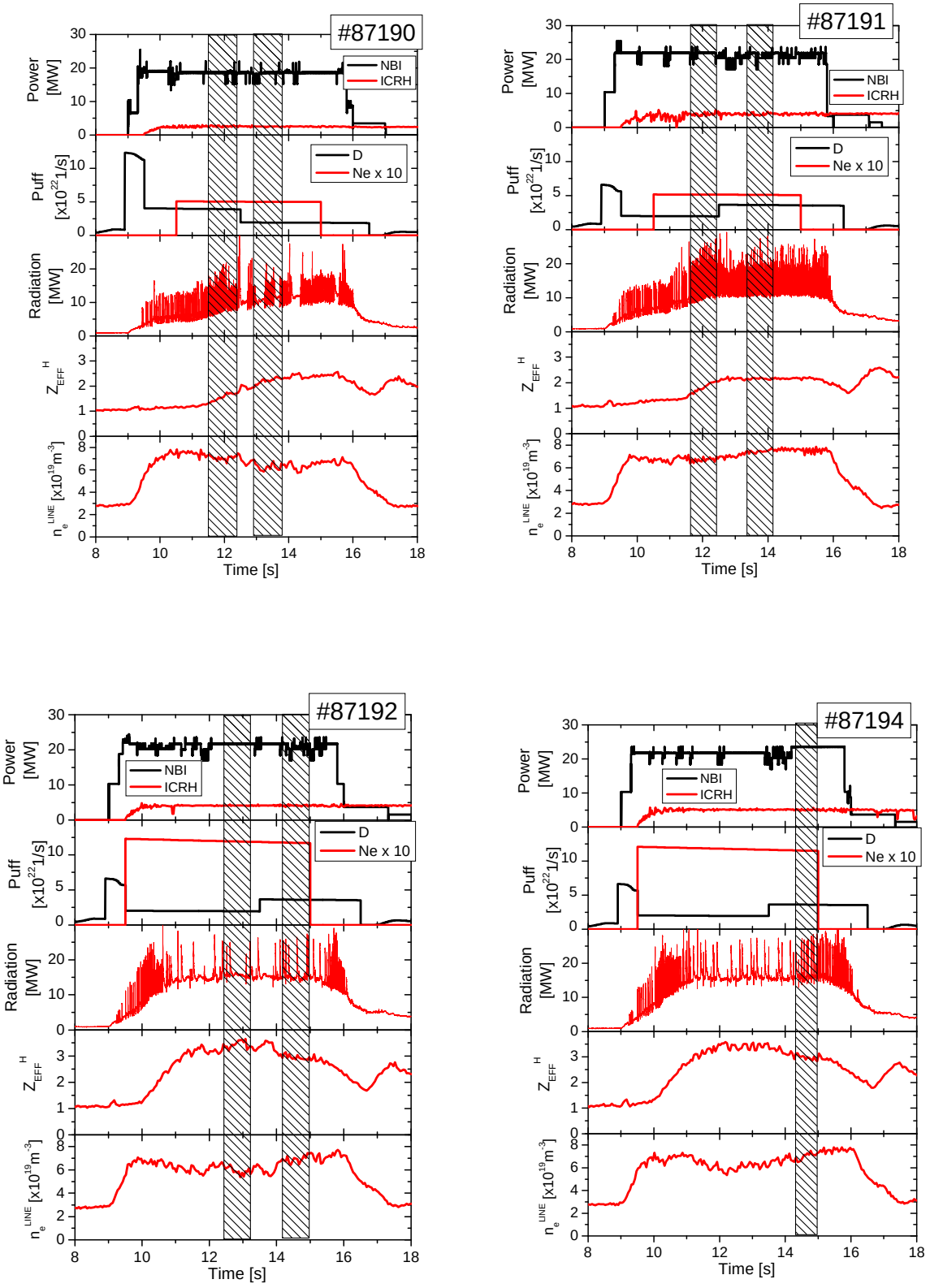
#87190
#87191
#87192
#87194
Power [MW]
NBI
ICRH
Puff [x10^22 1/s]
D
Ne x 10
Radiation [MW]
Z_EFF^H
n_e^LINE [x10^19 m^-3]
Time [s]

Fig. 1

P_{heat} [MW]	Γ_D [$x10^{22}$ 1/s]	Γ_{Ne} [$x10^{21}$ el/s]	$n_e(0)$ [$x10^{19}$ m^{-3}]	$T_e(0)$ keV	H_{98}	f_{RAD}	P_{RAD} [MW]	Z_{EFF} brem.	P_{DIV}/P_{TOT}	f_{ELM} [Hz]
22	3.6	5	8.3	3.5	0.68	0.47	10.4	1.9	0.42	40
	1.9	5	7.6	4.4	0.76	0.52	11.5	2.4	0.43	40/2
26.5	3.6	5	8.4	4.1	0.73	0.54	14.3	2.1	0.4	65
	1.9	5	8.0	4.4	0.68	0.47	12.3	2.0	0.35	60
26.5	3.6	12	8.0	5.3	0.79	0.57	15.2	3.0	0.39	9
	1.9	12	7.5	5.5	0.79	0.54	14.3	3.3	0.4	5
29.5	3.6	12	8.5	5.3	0.8	0.6	18.1	2.9	0.4	15

Table I. Summary of the experimental data

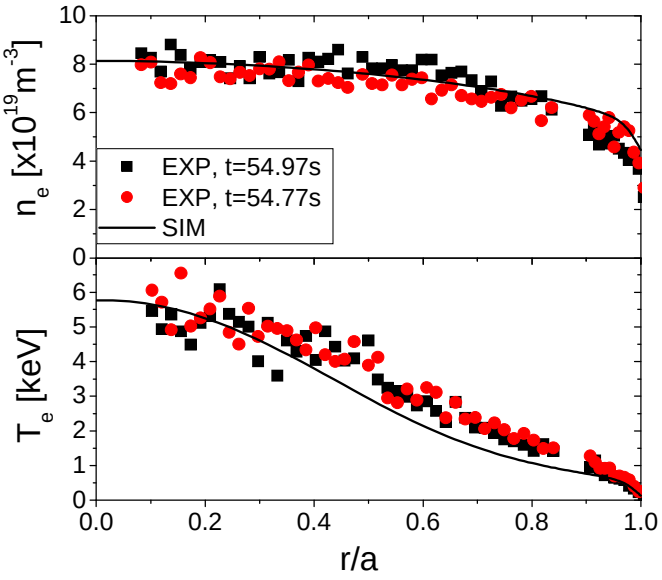

Fig. 2

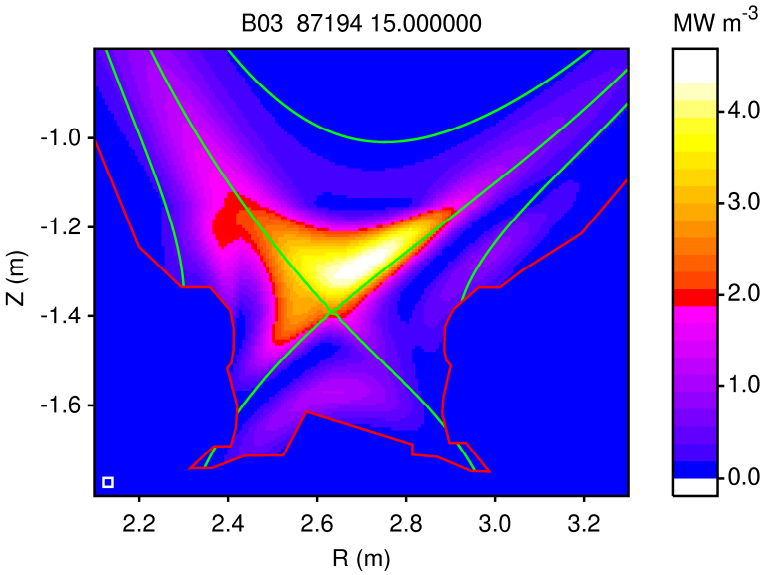
B03 87194 15.000000
MW m-3
4.0
3.0
2.0
1.0
0.0
-1.0
-1.2
-1.4
-1.6
Z (m)
2.2
2.4
2.6
2.8
3.0
3.2
R (m)

a)

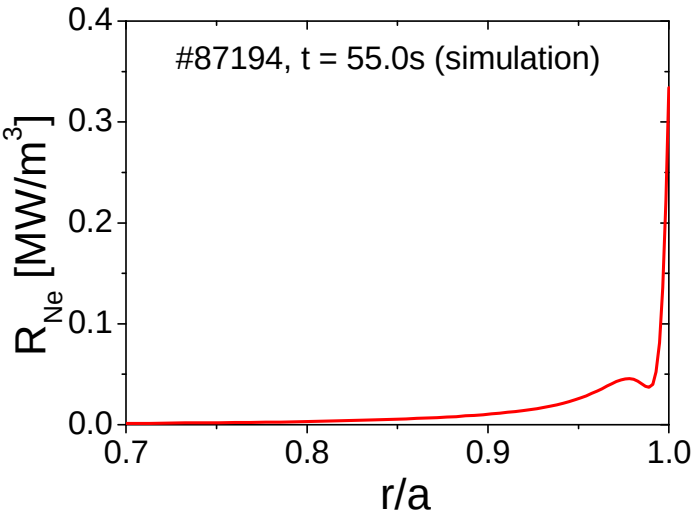
#87194, t = 55.0s (simulation)
0.4
0.3
0.2
0.1
0.0
R_Ne [MW/m3]
0.7
0.8
0.9
1.0
r/a

b)

Fig. 3

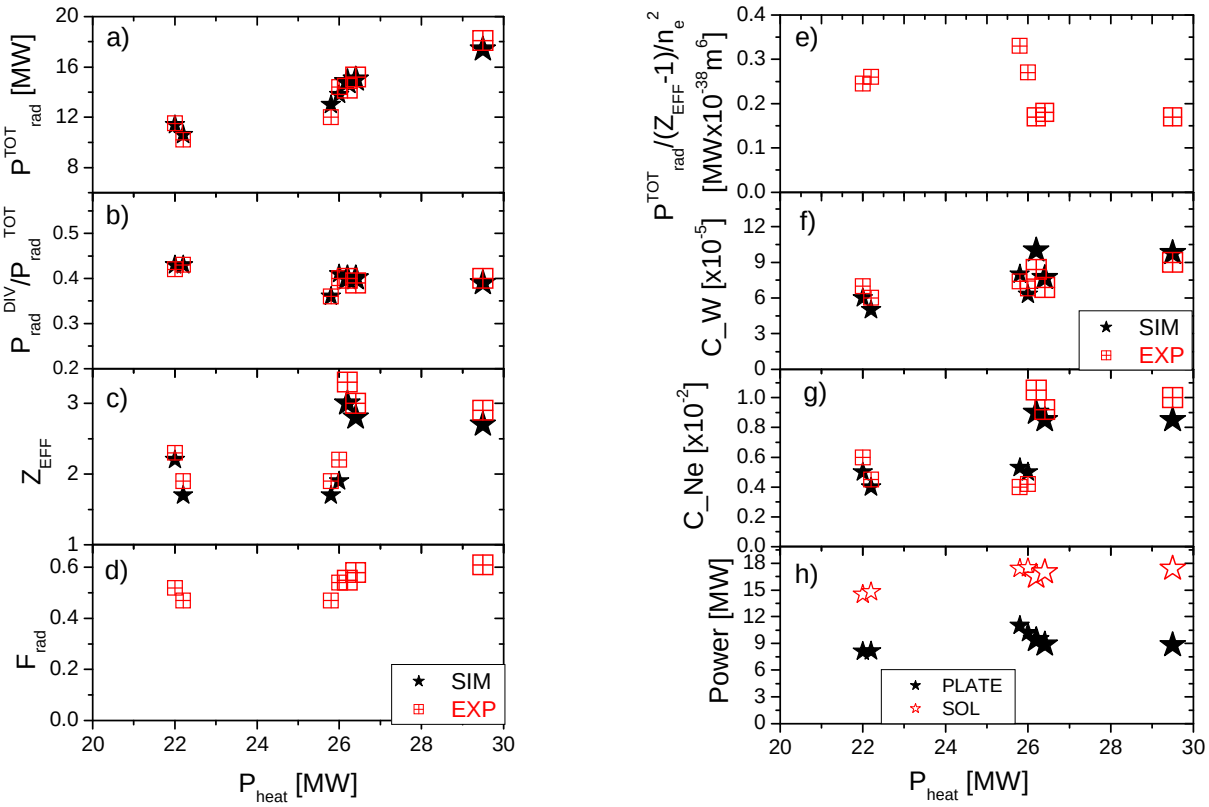

Fig. 4

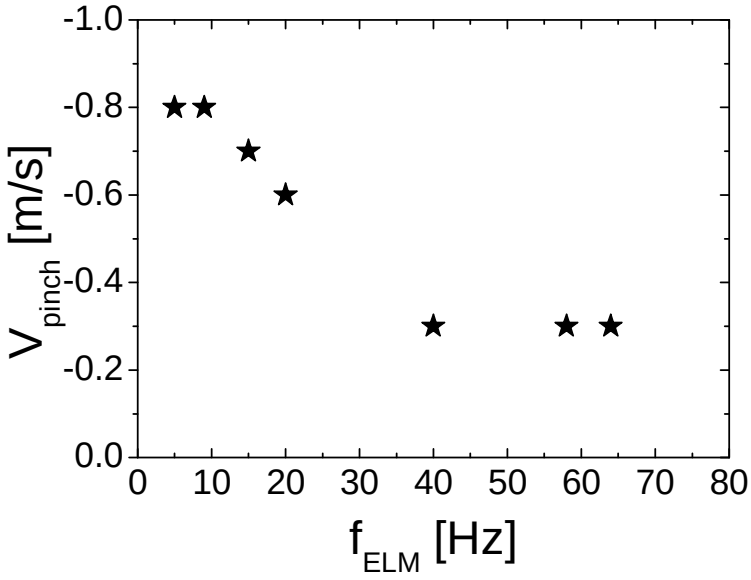
-1.0
-0.8
-0.6
-0.4
-0.2
0.0
V_pinch [m/s]
0
10
20
30
40
50
60
70
80
f_ELM [Hz]

Fig. 5a

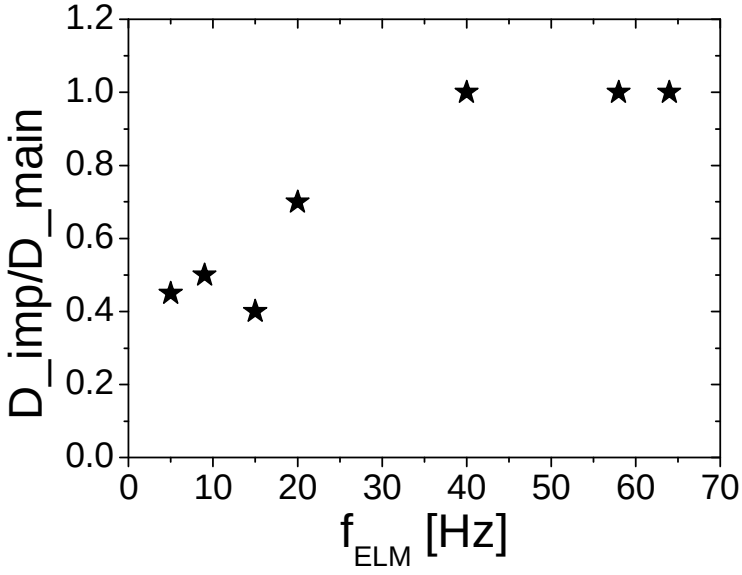
1.2
1.0
0.8
0.6
0.4
0.2
0.0
D_imp/D_main
0
10
20
30
40
50
60
70
f_ELM [Hz]

Fig. 5b

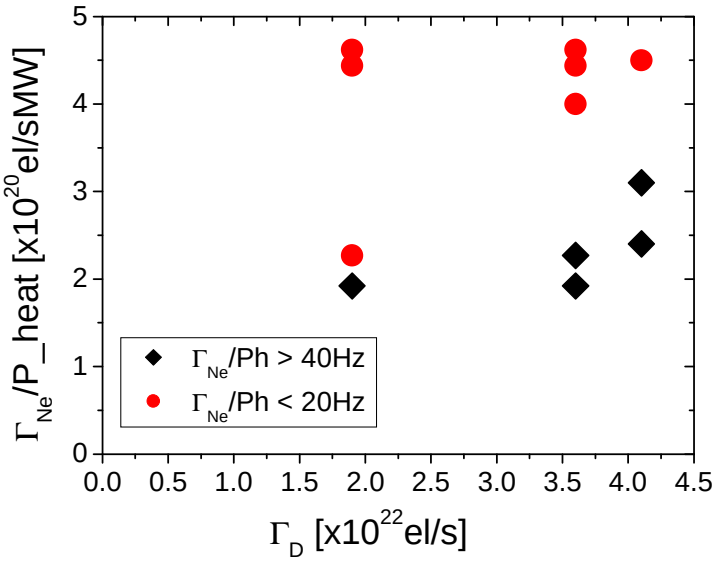
5
4
3
2
1
0
0.0
0.5
1.0
1.5
2.0
2.5
3.0
3.5
4.0
4.5
Γ_Ne/P_heat [x10^20 el/sMW]
Γ_D [x10^22 el/s]
Γ_Ne/Ph > 40Hz
Γ_Ne/Ph < 20Hz

Fig. 6